Planetary seismometry

Philippe Lognonné, W. Pike

1.3 **Planetary seismometry**

Philippe Lognonné (lognonne@ipgp.fr)
Université Paris Diderot -Sorbonne Paris Cité,
Institut de Physique du Globe de Paris, Paris, France

Tom Pike (w.t.pike@imperial.ac.uk)
Department of Electrical and Electronic Engineering
Imperial College, London, United Kingdom

Abstract: *We review briefly from the instrument and mission perspective the development of planetary seismometry. A first section describes the basic measurement principles of seismometers, as well as their limitations. This section includes also a description of the challenges due to technological constraints of space qualification. We then present and compare the different seismometers implemented on past missions, namely the series of lunar missions culminating in the Apollo seismic investigations and the past attempts to investigate the seismology of Mars. We review the current terrestrial seismic instrumentation and how techniques have been developed to isolate the seismic signal from all other sources. Finally we look forward to the future, nearer term with the seismic instrumentation on the InSight mission to Mars, and beyond to other seismic investigations throughout the solar system*.

1 The technical challenges of planetary seismometry

1.1 Basics of seismometry

Seismology is based on the recording, analysis and inversion of the seismic waves, and request therefore the measurement of these waves by instruments. Although being proposed and implemented in the early times of space exploration with the Ranger program (see section 2.1), it had to wait July 1969 for its first successful use in planetary exploration, with the installation of the Apollo 11 seismometer (Figure 1).

This instrument, like all seismometers, is an inertial system detecting the ground acceleration generated by the seismic waves. Strictly speaking, these inertial systems are not only detecting the ground acceleration, but the sum of all temporal changes of the gravity, which include those related to the ground relative acceleration plus the local gravity change due to the displacement of the sensor (horizontal tilt and free air anomaly) and the gravitational change due to global mass redistribution generated by seismic event and associated waves.

To achieve the detection of inertial acceleration, most of the seismic instruments are measuring the displacement or velocity of a mass suspended by a spring, with either velocity transducers based on coil/magnet system generating a an electromotive force, like geophones, or a displacement transducer based on capacitive or Linear Variable Differential Transformer displacement measurements, like the modern seismometers. Ground acceleration (or velocity) is then recovered through the instrument transfer function.

1.2 Instrumental noise limitations

The smallest seismic signal that can be detected by a seismometer is determined by the ability to resolve it above the aseismic background, which will inevitably also contribute to the recorded data. The lower this background, the better the performance of the instrument. This background, most often called the instrumental noise, can be divided into two contributions: the inherent noise generated by the instrument in the absence of any outside influences, commonly called the self noise, and the transduction of the aseismic signal which is produced by the unavoidable response of the instrument to non vibrational influences.

1.2.1 Instrument Self noise

The self-noise sets the ultimate performance of the instrument if a perfect deployment is possible which eliminates all aseismic influences. Planetary seismology is pushing instruments to this limits, as both the Apollo seismometers, deployed on the Moon and the Viking seismometer, deployed on Mars, have shown time periods during which no signal detection was made with amplitude larger than Instrument resolution. This is a major difference with Earth, which is a relatively seismically noisy object due to the ocean, atmosphere and human activity.

The thermodynamics of the system sets the largest contributions to the self-noise, with the two unavoidable contributions coming from the primary mechanical and (for all but direct write seismographs) the subsequent electronic transduction of the mechanical signal. Taking first the mechanical element, the external seismic vibration is transduced to a relative displacement or velocity of elements within the seismometer by a mass on a suspension. As the suspension will produce some finite energy losses, by the Fluctuation-Dissipation theorem (Callen and Welton, 1951) this will also produce random motion of the proof mass, known as the suspension noise. This white noise, with equal power density at all frequencies, is inversely proportional to the square root of the product of the proof mass, period and quality factor of the suspension. This immediately presents a challenge for any compact low-noise planetary seismometer, which will have to comply with restrictions in mass. Reducing the damping requires decisions about the materials of the suspension as well as gas damping of the motion of the proof mass.

The motion of the suspension is transduced electronically mainly through a capacitive displacement measurement (used for all planetary long period and the Short Period component of the InSight/Mars2016 NASA mission), of an electromagnetic velocity measurement (used all past Short Period instruments) or for higher frequencies piezo-electric measurements (used for the SESAME onboard the Rosetta/Philae lander, Kochan *et al.* 2000). Other displacement measurement have not yet been space qualified such as STS1-LVDT displacement, superconducting or optical sensing.

The second, electronic, contribution to the self-noise is most often set by the noise performance of the first amplifier used in the readout circuitry that makes this measurement. This amplifier noise is set in turn by its internal transistor technology, and as well as a broad band component also has a noise that increases at low frequencies, known as flicker noise. The latter can be avoided by modulating the readout circuitry at a frequency above where the flicker noise is dominant. However, the broad-band noise remains and its amplitude increases with the differential base

resistance and output loading of the first input transistor pairs of the amplifier, fundamentally as a product of the Fluctuation-Dissipation theorem.

Other contributions to the self noise include surface electric-field fluctuations on capacitive sensing plates (the "patch effect", Speake 1996), electromagnetic damping by eddy currents in conductive moving elements due to the instrument's own magnetic field, feedback noise, especially when integrators are used for correcting the diurnal large temperature variation and the reading noise, with both A/D noise and the one of output gain amplifiers. All these sources of noise must be tuned for the optimization of the instruments noise and performances of the space qualified components, most of the time more noisy than those used for Earth instrumentation.

1.2.2 Environmental noise limitations

Very large noise level differences are found on Earth with identical sensors due to the differences of the seismic vault used for the installation of these sensors: this variability is characterized by the High and Low noise models (Pedersen, 1993) for which 40-50 db of differences can be reported between the best and worst seismic stations. On the other hand, the noise recorded by the Apollo seismometers on the Moon, without atmosphere nor ocean, are extremely low for Earth standard and, except during Sun set or sun rise, are likely mainly related to the instrument noise. Lower noise on Earth are only found below 0.01 Hz and above 1 Hz, due to both better instruments at low and high frequencies and, on Earth, only in the best seismic vaults at long period and for buried stations at high frequencies.

These differences are mainly due to three sources of environmental noise: (i) noise generated directly in the sensor or on the sensor (ii) non seismic noise generated by the deformation of the ground supporting the sensor and (iii) continuous but uncoherent seismic waves detected by the sensor and generated very locally. Note that we do not consider here the uncoherent seismic waves called micro-seismic noise, generated remotely and now more and more used for seismic studies (e.g. Shapiro *et al*., 2005).

Let us first discuss (i) and therefore noise generated directly on the sensor. The largest is associated to temperature fluctuations, either originating from external temperature variations or from variations in the sensor heating or power dissipation. The temperature sensor sensitivity, typically between 10^{-5}-10^{-4} $ms^{-2}/°C$ is mainly related to the temperature dilatation of the instruments and, for the vertical or oblique seismometer counterbalancing the gravity at equilibrium, to the temperature sensitivity of the balancing forces (directly related to the dependence of the Young modulus of the spring for spring seismometers). Other temperature source of noise exists of course, like those related to electronics offset variations among others. In both case, the best mitigation of this noise is done with both thermal shielding and intrinsic compensation, the later based generally on self-compensated alloys for the spring and/or of thermal compensation mechanisms.

On Mars, like on any planets with atmosphere, pressure and wind generate also direct sensor noise. While the buoyancy pressure force on the proof mass can be cancelled by an vacuum or controlled atmosphere enclosure, the wind drag acting on the sensor structure and on the tether connecting the instrument with the lander request both a wind shield and a tether surface loop, especially due to the expected low rigidity of the Martian surface and displacements of the sensor related to these aseismic forces. Finally, magnetic field variations generate noise too on seismometers

with springs with non zero magnetostriction effects or with magnetic sensitivity related to motors magnets, or coils, as observed on the Apollo Short period seismometer during magnetic storms. Mitigation can be done either by mu-metal shielding, active compensation with Helmoltz coils or decorrelation (Forbriger *et al.*, 2010). Alternatively, this effect can be corrected through the additional measurement of magnetic field, as planned on the InSight mission.

Last but not least, other pressure induced signals will be, on Mars, related to the static loading of the surface by the atmosphere and even gravitational attraction of the atmosphere [Figure 2], and will request pressure decorrelation techniques, as already performed on Earth (e.g. Beauduin *et al.*, 1996). The amplitudes of these noises are estimated to a few 10^{-9} ms^{-2} $Hz^{-1/2}$ (Lognonné and Mosser, 1993, Lognonné et al., 2012) depending on the wind amplitude.

2. The Lunar golden age

2.1 From Rangers to Surveyor

Planetary seismology began in 1959 with the Ranger program. While the Ranger probes were designed for a hard landing on the Moon, a "survival sphere" designed to support a 3000 g impact contained a vertical-axis 3.4 kg seismometer with a natural frequency of 1 Hz designed by the California Institute of Technology [Figure 3a, Lehner et al., 1962]. All three Ranger probes carrying this package failed but the earth version of the seismometer is still commercially available (SS-1 seismometer from Kinemetrics)

A few years later, a three-axis long-period (LP) seismometer and a short-period (SP) vertical-axis seismometer, with a total mass of 11.5 kg was built in the Lamont Doherty Geological Laboratory [Sutton & Latham, 1964] for the Surveyor mission. Because of weight and power restrictions, this instrument was first descoped to a single SP seismometer and then cancelled. Both the LP and SP seismometers had to await the Apollo missions, but the groundwork had been done to provide high quality seismic instrumentation.

2.2 The Apollo Instruments

2.2.1 The Passive Seismic Experiment

The first successful installation of a seismometer on the Moon was achieved in July 1969, during the Apollo 11 mission (Figure 1). The Passive Seismic Experiment (PSE) based on the 11.5 kg Surveyor payload, consisted of a triaxial LP seismometer, with a natural period of 15 s, and an SP seismometer with a natural period of 1 s. PSE had a volume of 12 liters and a power consumption of between 4.3 and 7.4 W [Figure 3b, Latham et al. 1969]. It is notable that most of the structural elements were machined out of beryllium, with a much lower density (1850 kgm^{-3}) than other metals with comparable structural properties (e.g. titanium, 4400 kgm^{-3}) but this came with a very significant cost impact. These seismometers were extremely sensitive, capable of detecting a minimum signal of 300 pm for the LP in flat mode, 50 pm for the LP in peaked mode at 0.45 Hz and 50 pm for the SP seismometer at 8 Hz. The nominal response curves are shown in Figure 5.

A few months later Apollo 12 installed a new PSE station. This time, a radioactive thermal generator allowed continuous operation through the long lunar night (with thermal regulation keeping the temperature stable day and night) and the

deployment was performed more carefully (Figure 3). Other stations were deployed by Apollo 14, 15 and 16 to form a seismic network of four stations. All but the Apollo 12 SP seismometer and Apollo 14 vertical LP seismometer operated until the end of September 1977, when all were shut down from the Earth.

2.2.2 Other Apollo seismic instrumentation

Also deployed by Apollo were geophones, used for the Active Seismic Experiment on Apollo 14, 16 and 17. They had a flat velocity output from 8 Hz to about 100 Hz, and were operated at a sampling rate of 117.8 Hz. Their resolutions at 10 Hz were comparable to those of the PSE SP (with a system signal to noise of about 40 db at 10 Hz for a peak-to-peak signal of 1 nm). In addition the Apollo 17 gravimeter, initially dedicated to the search for gravitational waves, was able to function as a seismometer (Kawamura et al., 2010).

3.1 Viking

In 1976 the two Viking landers initiated the first seismic observations of Mars [Figure 3c, Anderson et al., 1977]. Only the Viking 2 lander's seismometer worked however, as the three components of the Viking 1 seismometer failed to uncage. The three-axis seismometer was an SP instrument, with a natural period of 0.25 s, a total mass of 2.2 kg, a volume of 1.4 liters and a nominal power consumption of 3.5 W. No recentering was necessary with a tilt range of 23 degrees. The sensitivity of this SP seismometer was ten times worth than the SP Apollo seismometer, for periods smaller than 1 s (Figure 5). The seismometers were mounted on the body of the lander, with coupling to the surface though the shock absorbers on the legs. A further limitation was the low telemetry data rate, considerably lower than Apollo's. Compression of data was thus necessary and most of the monitoring was done in Event mode, where the envelope of the seismic signal and the number of zero crossings was returned every 1.01 sec. No convincing event detection was performed during the 19 months of nearly continuous operation of the Viking Lander 2 seismometer and the data have been mainly used to constrain the wind on Mars.

3.2 Mars96

Twenty years later, the Mars 96 mission was expected to re-open the seismic exploration of Mars. The two small surface stations were equipped with an 0.1-1 Hz vertical seismometer (OPTIMISM experiment, Lognonné et al., 1996), integrated inside the small stations (Linkin *et al*., 1996) for thermal insulation reasons. These two stations were complemented by two penetrators equipped with very short period (100 Hz) vertical seismometers without unfortunately overlap with the OPTIMISM frequency band. Nevertheless, the Mars96 mission would have deployed the second operating seismic network on a terrestrial body if it had not been sadly lost shortly after its launch.

The design of the OPTIMISM seismometer was constrained by the very low power and mass allocation of the surface-station payload, as well as the high shock level of the landing. Among all the constraints, the most severe for OPTIMISM was the very low power allocated (50 mW), leading the instrument to use a dual transducer design: a low power velocity transducer for the bandwidth from 0.5-10s and a very low power displacement transducer for the control of the mass position, as well as for surface wave detection (5-50s). The pendulum was stored in a half-sphere made of titanium with automatic leveling (Figure 3d). Nevertheless OPTIMISM was expected to perform better than Viking (Figure 5) with only a mass of 405 g and a volume of one liter.

4. Current and future missions

4.1 Current instrumentation

Starting in the early 1990's a new generation of seismometers was developed for Mars with international efforts to gain approval for a Mars network missions, under the proposals Mesur, MarsNet, Intermarsnet, Impact, Netlander, amongst others (See Lognonné, 2005 for project references). Additional development was done in Japan for the Lunar-A penetrator mission (Shiraishi *et al*. 2008), cancelled in 2007. However it took two decades to see these efforts bear fruit with the selection by NASA of InSight (Banerdt et al., 2012) under the Discovery program.

Its single lander will be launched in March 2016, with a landing in late September 2016. As its prime payload element, SEIS, will be equipped with a dual VBB/SP 3 axis seismometer, together with a geodetic beacon (RISE), a heat flow experiment (HP3) and a set of environmental sensors (APSS), to support the seismic measurements. SEIS is lead by the French space Agency CNES and IPGP with contributions from UK, German, Swiss and US Space agencies and labs.

With only one lander, InSight will need to detect surface waves completing a full orbit around the planet, requiring a low instrument noise level, $< 10^{-9}$ $ms^{-2}/Hz^{1/2}$, in the bandwidth 0.01 to 0.05 Hz. The performance and installation quality of the InSight seismometer will therefore be critical parameters to ensure success with a sensitivity higher than previous Mars seismometers (see Figure 4 for comparison). SEIS also can expect a much better deployment with the InSight lander providing a robotic installation of SEIS from the deck of the lander down to the ground followed by the lowering of a wind and thermal shield (WTS). Figure 5c illustrates the level of thermal protection and shows the evacuated titanium sphere in which VBB sensors are located. In addition, a thermal blanket wrapped around both the VBB sphere and SPs and the WTS will provide additional shielding. All together, these three thermal barriers produce an effective time constant at low frequencies of between 2 and 5.5 hr. It is likely that SEIS will be close to the best deployment and sensitivity that can be achieved by a robotic installation on the surface of Mars.

Looking at the seismometers themselves, SEIS VBB (See Figure 6) is based around an inverted pendulum, with the gravity acting against the spring to lower the pendulum natural frequency to about 0.45Hz for a proof mass of 190 g. It uses a highly sensitive capacitive transducer to drive a feedback designed to provide response flat in ground velocity to within 10 dB from 50 to 0.5 s, with an expected noise below 10^{-9} m s^{-2} $Hz^{-1/2}$ between 0.01 and 2 Hz. The output is digitized at 24 bits, giving 10 dB headroom over the instrument noise floor at the same time as a saturation threshold larger than Viking.

SEIS SP (Figure 7) consists of a set of micromachined sensor heads, one vertical and two horizontal axes. The suspension and proof mass of each sensor are etched from single-crystal silicon wafers using deep reactive ion etching to produce a 7Hz suspension and a 0.4 g proof mass. Both the period and mass are much smaller than conventional seismometers, though at the limit of micromachined devices. The motion of the proof mass is capacitively measured by the change in overlap between an array of electrodes on the proof mass and an opposed fixed array connected to the outer frame of the suspension. This geometry has several advantages for planetary operation. As a much larger motion of the proof mass can be accommodated compared to more conventional capacitive transducers that sense a closing gap between their plates, the SP can be operated over a large tilt range of deployment.

Combined with the very low cross-axis compliance of the micromachined suspension this also allow SEIS SP to be fully tested on Earth under tilt conditions corresponding to Martian gravity. In addition, as sliding rather than squeeze-film gas damping occurs, a high quality factor of several hundred can be achieved without evacuation, giving an suspension Brownian noise of 4.5 10^{-9} $ms^{-2}Hz^{1/2}$ at 300K. SEIS SP's feedback produces a flat velocity output over a bandwidth from 40 Hz to below 0.1 Hz producing an overlap with the VBB, with a target acceleration sensitivity of below 5 x 10^{-9} ms^{-2} $Hz^{-1/2}$.

4.2 Future seismic projects and instrumentation directions

The next decades' seismic projects will likely focus on return opportunities to the Moon and network opportunities on Mars alongside even more challenging deployments, such as Venus and Europa. While several seismic payloads have recently studied for the Moon (JAXA/SELENE2, Tanaka *et al*., 2013; NASA/Lunette, Neal *et al*., 2011, ESA/FarSide, Mimoun *et al*., 2012, ESA/Lunar Net, Smith *et al*, 2012) Mars (ESA/INSPIRE, Chicarro, 2013) or Europa (Gowen *et al*., 2011), only SELENE2 has gone through a full mission definition phase, though unfortunately not progressing further.

For these projects, the two major directions in term of new instrumentation development are mainly mass/cost reduction for network missions and, for the Moon, developing the performance beyond Apollo required to completely elucidate the deep interior structure (Yamada *et al.*, 2013).

One mission approach that aims to greatly reduce costs below a conventional soft landing is the deployment of networks of seismometers using penetrators. These have the advantage of producing excellent coupling to the subsurface, while reducing environmental noise, but place severe constraints on instrumentation, particularly the suspension of a seismometer. A micromachined seismometer, with its small proof mass, can be armoured against high shocks. One approach, similar to the one used on the Ranger seismometer (Lehner *et al*. 1962) is to encase the suspension in a sublimable wax that cleanly dissipates after deployment, and has been demonstrated for shocks up to 14,000g. Another is to allow free motion of the proof mass but incorporate solder buffers to replace brittle with ductile contact at the extremes of motion. Such suspensions can survive drop tests to 5,000g.

While the determination of the level of the ambient seismic floor of Mars is awaiting the first data from the InSight seismometers, it appears that the Apollo seismometers may not have reached the lunar seismic floor (Lognonné *et al*. 2009) with the ambient level possibly 100 times smaller than the Apollo resolution, perhaps 10^{-12}-10^{-11} ms^{-2} $Hz^{-1/2}$ from 0.1 to 1Hz and even less at longer periods. Such a very low level would open up new perspectives in lunar seismology, including detection of gravitational waves, as envisaged for the Apollo 17 gravimeter, or even impacts of strange matter (e.g. Banerdt *et al*., 2007). The corresponding demands on the instrumentation are high with either superconducting quantum displacement sensing (Paik *et al*., 2009) or possibly optical detection schemes (e.g. Zumberge *et al*., 2010) offering the required sensitivity, with the latter giving the advantage of mass reduction through operation without feedback and fine leveling.

Landing on planets will however always increase significantly the cost of future projects, and remote sensing seismometry on telluric planets (see section 4.4 for remote sensing seismology on giant planets) might be important for Venus, where

surface seismic operation is extremely challenging, as well as airless bodies. For the latter case, the lack of atmospheric/ionospheric noise in the signal path between orbiting satellites and surface beacons or reflectors can give a resolution at the micrometer level, which would correspond to a ground acceleration of 2×10^{-10} ms^{-2} at 500 s, comparable to a surface-deployed seismometer. This might enable measurements of normal modes, surface waves and even large quakes from space and has been proposed for Europe using radar ranging (Panning *et al.*, 2006). In contrast for Venus the thick atmosphere and resultant large coupling between the planet's interior and atmosphere (Garcia *et al.*, 2005, Lognonné and Johnson, 2007) offers the possibility of detecting the surface waves of quakes through induced vertical ionosphere oscillations, in ways similar to those now done routinely on Earth with Doppler sounding (e.g. Artru *et al.*, 2004), but with attenuation short period limitation due to the CO_2 atmosphere (Garcia *et al.*, 2005).

5 References

Anderson, D. L., Miller, W. F., Latham, G. V. *et al.* (1977). Seismology on Mars. *J. Geophys. Res.*, **82**, 4524-46.

Artru, J., T. Farges, T., Lognonné, P. (2004). Acoustic waves generated from seismic surface waves: propagation properties determined from Doppler sounding observation and normal-modes modeling. *Geophys. J. Int.*, **158**, 1067-1077.

Banerdt, W. B; Chui, T., Griggs, C. E. *et al*. (2007). Using the Moon as a low-noise seismic detector for strange quark nuggets, Nuclear *Physics B Proceedings Supplements*, **166**, 203-208.

Banerdt, W. B., Smrekar, S., Alkalai, L. *et al.* (2012). InSight: An Integrated Exploration of the Interior of Mars, 43rd Lunar and Planetary Science Conference, held March 19–23, 2012 at The Woodlands, Texas. LPI Contribution No. 1659.

Beauduin, R., Lognonné, P., Montagner, J.P., Cacho, S., Karczewski, J.F. and Morand, M. (1996). The effect of the atmospheric pressure changes on seismic signals or how to improve the quality of a station, *Bull. Seism. Soc. Am.*, **86**, 1760-1769.

Callen, H. B. and Welton, T. A. (1951). Irreversibility and Generalized Noise, *Physical Review*, **83**, 34-40

Chicarro, A. F. (2013). INSPIRE — A Future European Mars Network Science Mission, 44th Lunar and Planetary Science Conference, held March 18-22, 2013 in The Woodlands, Texas. LPI Contribution No. 1719.

Forbriger, T, Widmer-Schnidrig, R., Wielandt, E., Hayman, M., Ackerley, N. (2010). Magnetic field background variations can limit the resolution of seismic broad-band sensors, *Geophys. J. Int,*, **183**, 303-312.

Garcia, R, Lognonné, P, Bonnin, X. (2005). Detecting atmospheric perturbations produced by Venus quakes. *Geophys. Res. Lett.*, **32**, L16205

Gowen, R. A., Smith, A., Fortes, A. D. *et al.* (2011). Penetrators for in situ subsurface investigations of Europa, *Advances in Space Research*, **48**, 725-742.

Kawamura, T., Tanaka, S., Kobayashi, N., Lognonné, P. (2010). The Lunar Surface Gravimeter as a Lunar Seismometer, Ground-Based Geophysics on the Moon, January 21-22, 2010, held in Tempe, Arizona. LPI Contribution No. 1530.

Kochan, H., Feibig, W., Konopka, U. *et al.* (2000). CASSE -- The ROSETTA lander comet acoustic surface sounding experiment -- status of some aspects, the technical realisation and laboratory simulations. *Planet. Space Sci.*, **48**, 385-99.

Latham, G. V., Ewing, M., Press, F. and Sutton, G. (1969). Passive seismic experiment. *Science*, **165**, 241-250.

Lehner, F. E., Witt, E. O., Miller, W. F. and Gurney, R. D. (1962). A seismometer for lunar experiments. *J. Geophys. Res.,* **67**, 4779-86.

Linkin, V. , Harri, A. M., Lipatov, A. et al. (1998). A sophisticated lander for scientific exploration of Mars: Scientific objectives and Implementation of the Mars96 Small Station, *Planet. Space Sci.*, **46**, 717-737.

Lognonné, P (2005). Planetary seismology, *Annual Review in Earth Planet Sci* , **33**, 191-1934.

Lognonné, P and Mosser, B. (1993). Planetary Seismology, *Survey in Geophysic*, **14**, 239-302.

Lognonné, P , Zharkov, V.N., Karczewski, J.K. *et al.* (1998). The Seismic Optimism Experiment, *Planet. Space Sci*, **46**, *739-747*.

Lognonné, P and C Johnson, C. L. (2007). Planetary Seismology, in *Treatise on Geophysics*, 10, Planets and Moons », editor G Shubert, chapter 4, 69-122, Elsevier.

Lognonné, P, LeFeuvre, M., Johnson, C. L. and R C Weber, R. C. (2009). Moon meteoritic seismic hum: steady state prediction, *J Geophys Res*, **114**, E12003.

Lognonné, P., Spiga, A., Hurst, K. *et al.* (2012) Martian Atmospheric Induced Micro-Seismic Noise Generation: Large Eddy Simulations, 43rd Lunar and Planetary Science Conference, held March 19–23, 2012 at The Woodlands, Texas LPI Contribution No 1659.

Mimoun, D., Wieczorek, M., Alkalai, L. *et al.* (2012). Farside explorer: unique science from a mission to the farside of the moon *Experimental Astronomy* , **33**, 529-585

Neal, C. R., Banerdt, W. B., Alkalai, L. *et al.* (2011). Lunette: A Two-Lander Discovery-Class Geophysics Mission to the Moon, 42nd Lunar and Planetary Science Conference, held March 7-11, 2011 at The Woodlands, Texas LPI Contribution No 1608.

Pedersen, J. (1993). Observation and modeling of seismic background noise, *U S Geol Surv Open-file Rep* , **93-322**, 1-45

Paik, H. J., Venkateswara, K. Y. (2009). Gravitational wave detection on the Moon and the moons of Mars, *Advances in Space Research*, **43**, 167-170

Panning, M., Lekic, V., Manga, M., Cammarano, F., Romanowicz, B. (2006). Long-period seismology on Europa: 2 Predicted seismic response, *J Geophys Res* , **111**, CiteID E12008

Shiraishi, H., Tanaka, S., Fujimura, A., Hayakawa, H. (2008). The present status of the Japanese Penetrator Mission: LUNAR-A, Advances in Space Research, **42**, 386-393

Shapiro, N.M., Campillo, M., Rittzwoller M.H., Michael, H, (2005). High-resolution surface-wave tomography from ambient seismic noise, *Science*, **307**, 1615-18

Smith, A., Crawford, I. A., Gowen, R. A. *et al.* (2009). Lunar Net—a proposal in response to an ESA M3 call in 2010 for a medium sized mission. *Experimental Astronomy*, **33,** 587-644

Speake, C. C. (1996). Forces and force gradients due to patch fields and contact-potential differences, *Classical and Quantum Gravity*, **13**, A291-A297

Sutton, G. H., Latham, G. V. (1964). Analysis of a feedback controlled seismometer, *J. Geophys Res* , **69**, 3865- 82

Tanaka, S., Mitani, T., Otake, H. *et al.* (2013). Present Status of the Lunar Lander Project SELENE-2, 44th Lunar and Planetary Science Conference, held March 18-22, 2013 in The Woodlands, Texas LPI Contribution No 1719.

Yamada, R., Garcia, R. F. , Lognonné, P et al. (2013). On the possibility of lunar core phase detection using new seismometers for soft-landers in future lunar missions, *Planet Space Sci* , **81**, 18-31.

Zumberge, M., Berger, J., Otero, J., Wielandt, E. (2010). An Optical Seismometer without Force, *Bull Seismological Soc of America*, **100**, 598-605

Figure 1: Installation of the Apollo 11 seismometer by Buzz Aldrin. This first experiment was powered by solar panel power supply, while all next ones were by Radio Thermal Generator. It worked during day time of the first lunation, restarted at sun rise of the second lunation and stopped 9 days later, with a total of 21 days of operation [Latham et al , 1969].

Figure 2: The detectability of normal modes for large quakes on Mars is shown in this plot of the calculated acceleration amplitude spectrum (black) for a quake with seismic moment 2×10^{17} Nm compared to SEIS/INSIGHT required (red) and expected (red dashed) sensitivity. Epicentral distance is 90 degrees. Also shown are modeled environmental noise sources included in the red dashed curves: thermal (cyan); atmospheric pressure (green); atmospheric gravity (blue).

Figure 3: Launched Missions with the corresponding number of instruments (inst.) deployed in different locations, with from top to bottom Rangers (3 inst.), Apollo PSE (5 inst.) , Viking (2 inst.), Mars96/Small Surface Stations (2 inst., mounted by the top on the lander structure). Numbers in quote indicate the number of Instruments deployed during the program or by the mission. Not shown are the Apollo Active Seismic experiments, the Mars 96 penetrators and the Rosetta Lander Philae, all with short period or ultra-short period instruments and the Apollo 17 gravimeter on the other frequency end. Note the different strategy for the instrument installation on the robotic missions: Ejection of a seismometer "ball" prior the crash for Ranger, Lander deck mounting for the Viking or Inside Lander mounting for the Mars 96. The Apollo seismometer (here a PSE unit in the collection of National Air and Space Museum) was installed by Astronauts and covered by a Thermal shield after proper leveling and orientation.

Figure 4: Response curves of the past (a, left) Mars and (b, middle) Moon seismometers. Figure (a) shows the resolution of the Viking seismometer in High data rate mode, the Optimism seismometer, in the long period position mode (POS), in the velocity mode OPTVIT1 at 1 Hz sampling rate and at 4 Hz (OPT VIT4). The figure shows also the expected resolution of the InSight seismometers, defined here as the RMS in 1/6 of a decade (equal roughly to the product of $0.62 \times ASD \times \sqrt{f}$ where ASD is the amplitude spectral density in $ms^{-2}\ Hz^{-1/2}$ and f the frequency). The two first are the velocity flat and acceleration flat outputs of the VBB sensors (VBB and POS) while the third one is the velocity flat output of the short-period (SP) instrument respectively. VBB's components are sensitive to acceleration along an oblique about 30° with respect to horizontal, while the SP are either vertical or horizontal. At 1 Hz, the expected resolution of the InSight VBB sensor is expected to be 10^3 times better than Viking. Figure (b) shows the Moon case, with the long (RA LP) and short (RA SP) period analog outputs of the Ranger seismometer, the Flat (AP LPF) and peaked (AP LPP) mode of the Apollo LP seismometer and the short period seismometer (AP SP). The transfer functions shown are the generic one. Figure (c) shows different sources and levels of seismic noise. The noise levels recorded on the Moon by the different

channels of the Apollo seismometers are compared with the earth-based Low Noise model of Pedersen (1993). Noise levels are from Apollo 12 vertical long period flat (AP Z LPF) mode and from Apollo 14 vertical short period (AP Z SP). These noise levels are likely an upper estimate of the Moon noise and may be related to the instruments. For the other components, note that the peaks near 0.45Hz of the peaked vertical (AP Z LPPG) and horizontal (AP H LP) peaked records might be related to differences between the Apollo 12 transfer function at the time of the recording and the pre-flight generic transfer function. The noise corresponding to the curve AP Z LPPC is obtained by changing the feedback parameters in order to minimize the noise peak (about 10% for the parameter K2 and h, see the Apollo transfer function at http://darts jaxa jp/planet/seismology/apollo/The Apollo Seismometer Responses pdf).

Figure 5: Past or current projects, again with the number of instruments expected. On the top, Lunar-A (2 inst.). On the middle, Netlander (4 inst.), both cancelled and respectively toward the Moon and Mars. On the bottom, the single station InSight SEIS system, which enclose both the VBB and the SP axis and with launch in 2016. Note the differences in the deployment strategy. Lunar-A is based on penetrators penetrating the ground and enabling a buried configuration for the seismometers, while both Netlander and InSight are based on a surface deployment. The major differences between the latter two is the much superior control of the installation for InSight, which uses a robotic arm and cover the instrument by a windshield while on Netlander, the seismometer legs are deployed to the surface through holes in the lander base, without any choice in the placement. The seismometer was however expected to be mechanically decoupled from the lander after deployment and was protected from wind/temperature by the lander structure.

Figure 6: The INSIGHT VBB sensor. Note the Earth counter mass, at the left, used on Earth to compensate the larger Earth gravity. This mass, removed for the Mars flight configuration, allows full tests on Earth.

Figure 7: The micromachined sensor of the short period seismometer of InSight SEIS instrument.

Picture origin and acknowledgements:
NASA: Figures 1, 3a-c, 3b top and bottom 5c.; IPGP, SODERN and CNES: Figure 3d, 5b and 6; CNES/J.Chetrit : Figure 5c-top; DLR and CNES: top Figure 5b; ISAS: Figure 5a
IC: Figure 7; National Air and Space Museum/Allan Needel : Figure 3b.

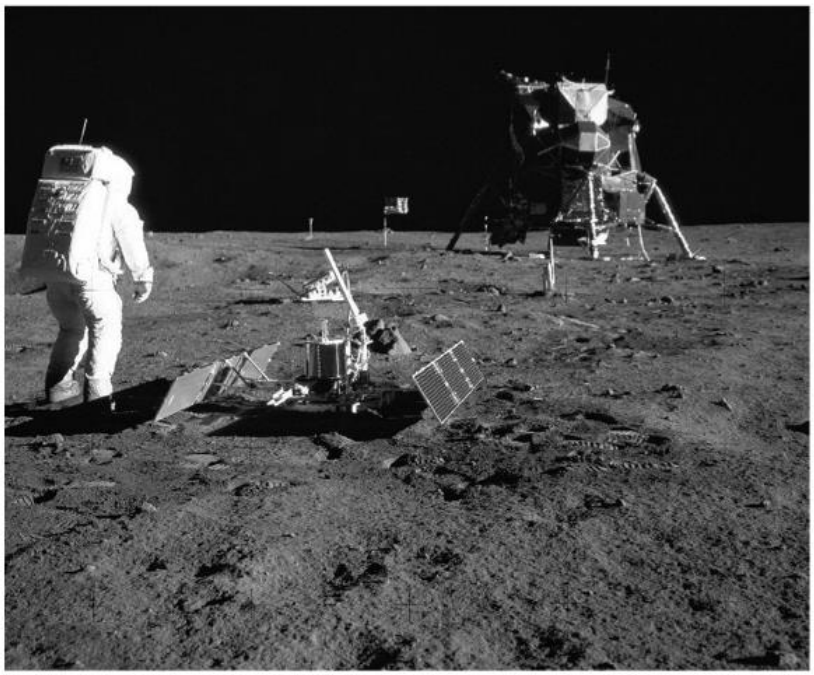

Figure 1

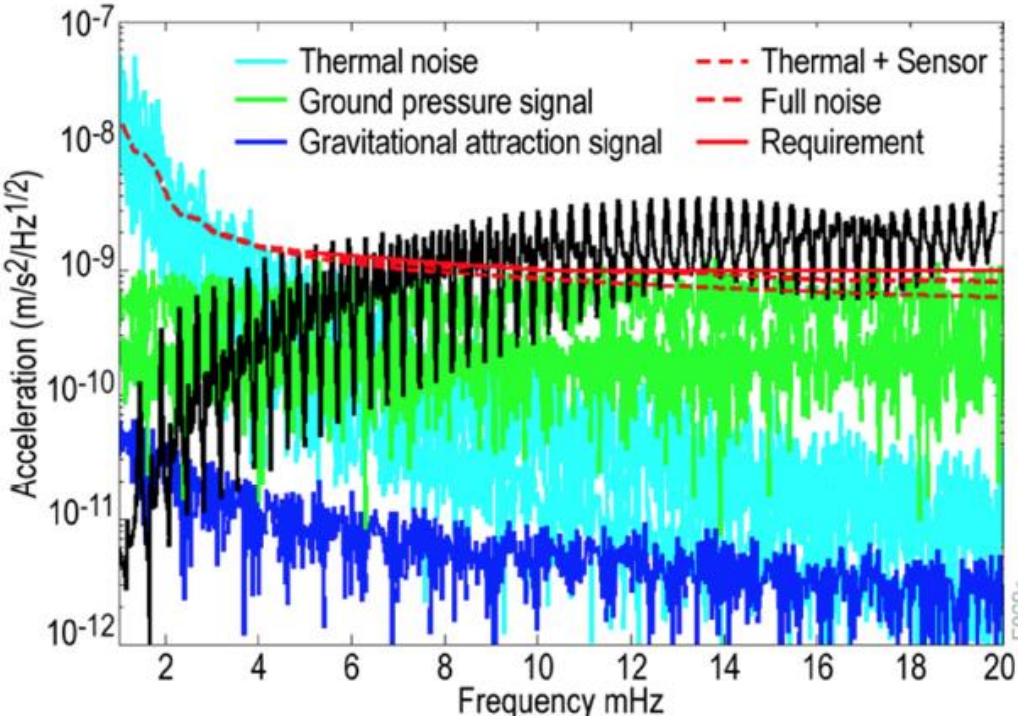

Figure 2

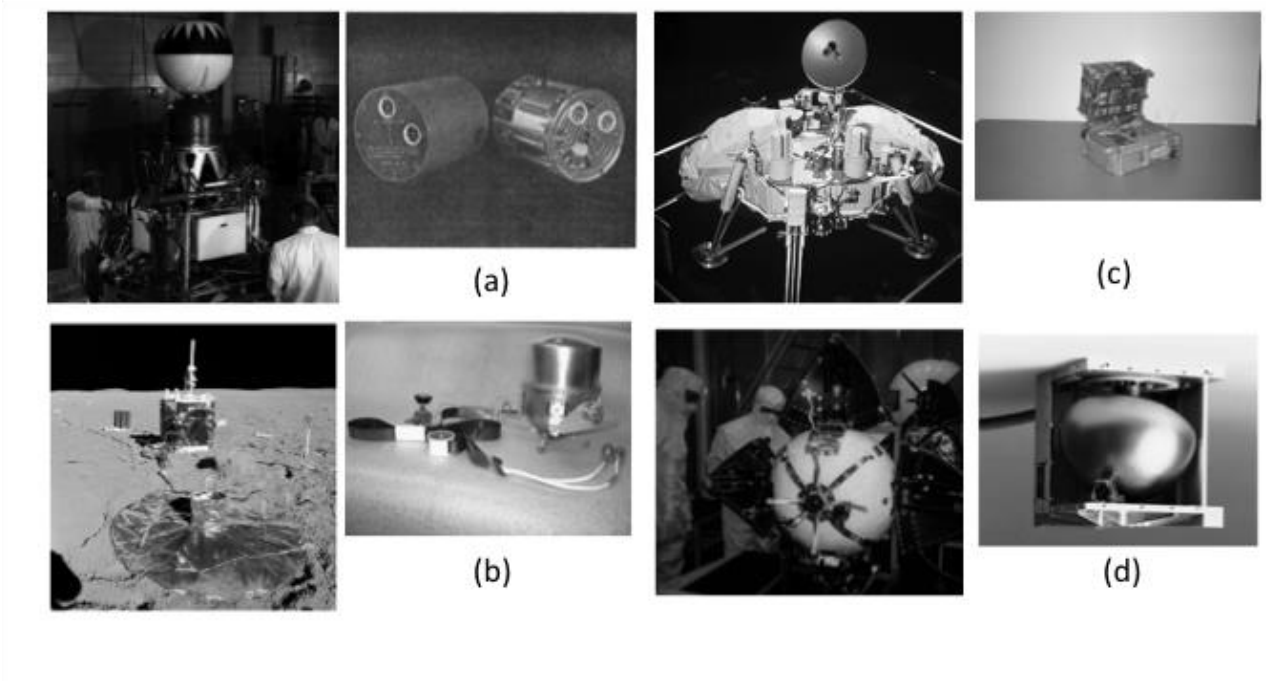

Figure 3

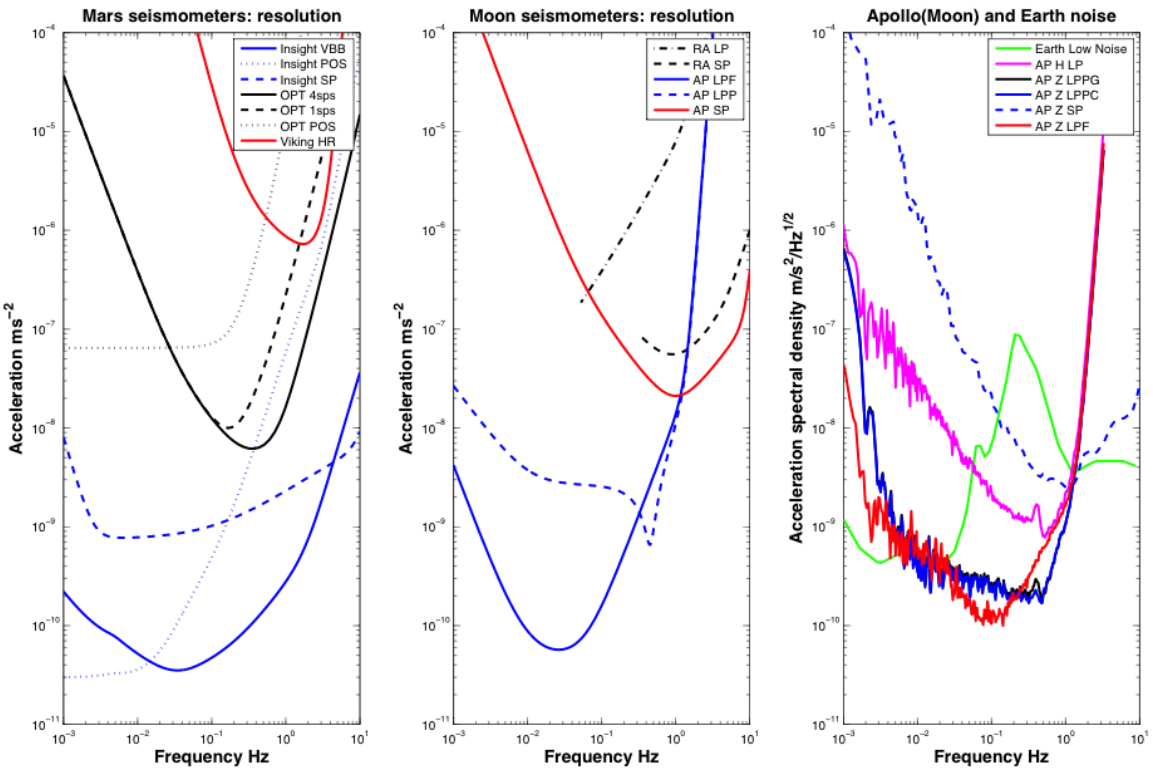

Figure 4

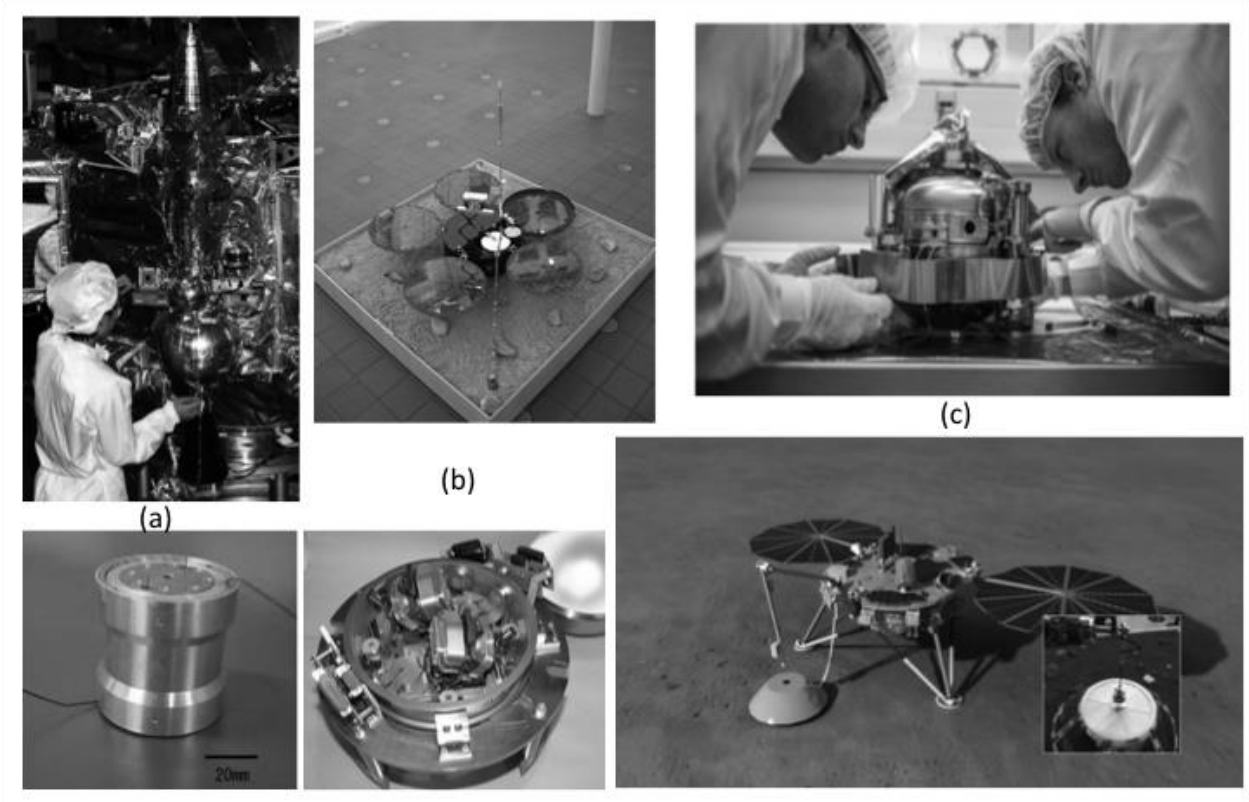

Figure 5

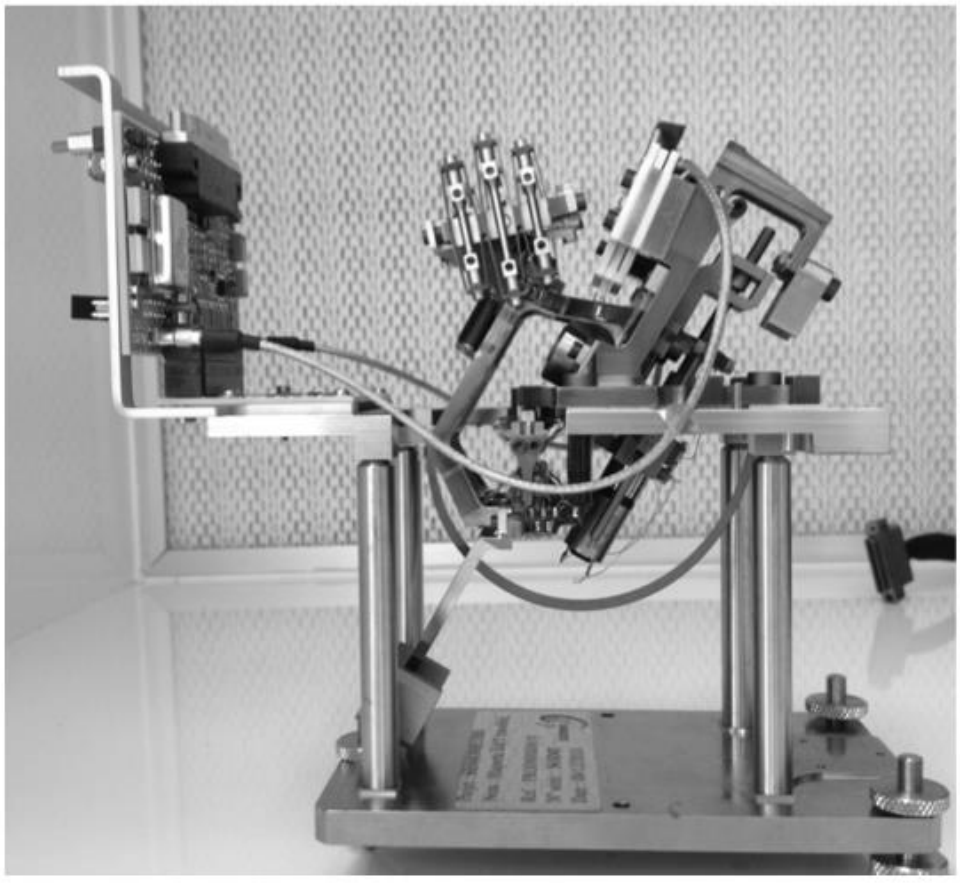

Figure 6

Figure 7